A Pain in the Neck: A Modeling Analysis for Design Limitations of Head Supported Mass

C. P. Eckersley[1], C. A. Cox[1], M. A. Ortiz-Paparoni[1], R. H. Lutz[2], T. C. Sell[3], and C. R. Bass[1]
[1] Injury Biomechanics Laboratory, Duke University; [2] Duke University Medical Center, Primary Care Sports Medicine; [3]Michael W. Krzyzewski Human Performance Laboratory

ABSTRACT

Head supported mass, including helmets, night vision, communications, and other attachments, is a two-edged sword. Though such technologies generally increase soldier survivability, there are functional occupational limits to how much mass may be borne effectively and safely. The chronic effects of an increased head supported mass include acute and degenerative cervical spine injuries. To understand the role this increased mass plays in chronic cervical spine injuries, the sensitivity of intervertebral stresses to the location and magnitude of the head supported mass was assessed using the Duke University Human and Neck Model (DUHNM). The DUHNM is a hybrid multibody and finite element model equipped with active musculature and anatomically accurate stiffness of spinal units. The region of interest included head supported mass from 0 to 5 kg at locations 0-100 mm from the head center of gravity in the vertical and horizontal directions. Simulations include the effects of running (~1 g-1 Hz sinusoidal input), jumping from low height (4 g-100 ms half sine input), and parachute drops (~10 g-50 ms half sine input) on maximum neck forces and moments. Extreme scenarios show increasing mass as well as the distance anterior the center of gravity increase the maximum moment and force in the neck by nearly an order of magnitude. Based on these simulations, we provide initial contours for design guidance envelopes for head supported mass and center of gravity location in terms of career longevity and assumed occupational scenarios for head supported mass under repeated impact loading.

INTRODUCTION

Increasing battle field head supported technologies has led to an increase in the head supported mass carried by soldiers, and there are functional occupational limits to the amount of head supported mass that can be borne effectively and safely (Butler, 1996, Manoogian, 2005, Bass, 2006, Manoogian, 2006). Because of this, the US Army sponsored a series of research projects investigating the role of head supported mass in helicopter pilot cervical spine injuries (Butler, 1996, Manoogian, 2005, Bass, 2006, Manoogian, 2006). It was hypothesized that helicopter vibrational input was producing higher cyclic cervical spine loads in pilots. The results of these studies supplied design guidelines for helicopter helmets and communication systems (Butler, 1996, Manoogian, 2005, Bass, 2006, Manoogian, 2006); however the conclusions were incomplete for two reasons: they did not apply to a broad enough population, and they only analyzed changes in head dynamics.

Recent epidemiological data suggest that chronic cervical spine injuries occur in other military groups that use head supported technologies, such as Special Operations Combat Soldiers and Sailors (Schoenfeld, 2012, Eagle, 2017). There are a variety of other inputs these groups are commonly exposed to such as jogging, jumping off of ledges, and parachute opening shocks that lead to increased cervical spine loads from a head supported mass. In addition, the ground panoramic night vision goggle system in use is larger and heavier than systems used in aviation.

Previous studies analyzing the role of head supported mass in repetitive loading used changes in head kinematics as the metric of interest (Butler, 1996, Manoogian, 2005, Manoogian, 2006). Preliminary work conducted in the Duke University Injury Biomechanics Laboratory has shown that in a number of occupational scenarios, cervical musculature activation will compensate for the addition of head supported mass and maintain head kinematics as if the increased load were not present (cf. (Pozzo, 1989)). Furthermore, static activation of cervical musculature that does not alter head kinematics can increase cervical spine loads to 40% of acute failure loads (Dibb, 2013).

This study analyzed the repeated intervertebral stresses resulting from an increased head supported mass, and investigated the role of these repetitive stresses in chronic cervical spine injuries. The value of head supported mass and the applied location were analyzed in this study. This analysis included both static and dynamic scenarios. The study used a hybrid multibody and finite element model enabling the measurement of intervertebral stresses and input conditions not possible with human subjects in a controlled experimental setting. Since there are no available injury criterion for chronic cervical spine injuries due to repetitive loading, work analyzing the role of repetitive loading in endplate fractures of the lumbar spine was used to gauge injury risk.

First of several hypothesis was the intervertebral forces generated by the cervical musculature to support the head in the static scenario will be a significant portion of the overall force generated in the dynamic scenarios. Next, increasing the distance of the head supported center of mass from the head center of gravity (CG) will increase the dynamic intervertebral forces. Finally, intervertebral stresses from increased head supported mass will be high enough to indicate the potential for injury due to repetitive loading. This work provides the initial foundation for design guidance envelopes for head supported mass and center of gravity location in terms of career longevity and assumed occupational scenarios under repeated impact loading.

METHODS

Model and Modeling Environment

Simulations, pre/post processing, and optimization analysis of the models was conducted in LS-DYNA, LS-PrePost, and LS-OPT (Livermore Software Technology Corporation, Livermore CA) respectively. The Duke University Human Neck Model (DUHNM) developed by the Duke University Injury Biomechanics Laboratory served as the computational human surrogate. This model consists of an osteoligamentous spine as well as 23 active muscle pairs acting along anatomically accurate paths (Camacho, 1997, Van Ee, 2000, Chancey, 2003, Dibb, 2013, Dibb, 2014). The seven vertebrae (C1C2-T1) are modeled as rigid bodies, while the intervertebral disks (OC2-C7T1 are represented by non-linear six degree of freedom springs in parallel with linear dampers, and positioned according to literature (Dvorak, 1991, Van Mameren, 1992, Chancey, 2007). The model has been validated with post mortem human subject (PMHS) data in compression, tension, flexion, and extension in the midsagittal plane. It has also been dynamically validated against frontal impact data from the Naval BioDynamics Lab (NBDL) and the Children's Hospital of Philadelphia (CHOP) (Ewing, 1972, Arbogast, 2009, Dibb, 2011, Dibb, 2013, Dibb, 2014). Figure 1 depicts the model neck connected to a head designed as a rigid body that mimics the mass and inertial properties of a human head. A point mass was used to represent the head supported mass. This could then be moved to the desired center of mass of the head supported mass and rigidly connected to the skull to account for the additional mass and inertial properties.

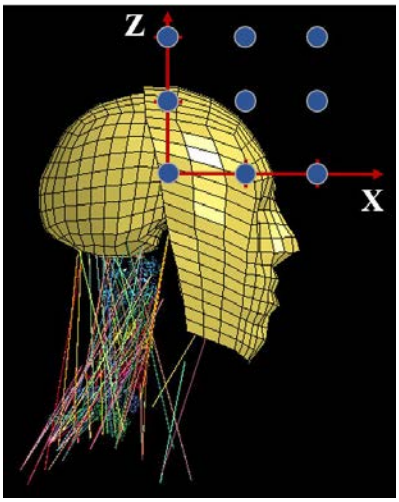

Figure 1: Illustration of the head and neck model used for simulation and the locations where additional mass was added. The axis originates at the CG of the head and the tick marks are 0.05 and 0.1 m from the CG. These values were selected to cover the range of potential head supported masses and locations.

Static Optimization Simulations

The test matrix for static optimization analysis used masses of 0, 3, and 5 kg located at combinations of 0.0, 0.05 and 0.1 m from the head CG as seen in Figure 1. To begin optimization, muscle activation states were set to a relaxed neck position, and in order to reduce the sample space and overall computation time, only the six main flexor and extensor muscle activation levels were modulated (Longus Capitis, Sternocleidomastoid, Splenius Capitis, Splenius Cervicis, and Trapezius) (Dibb, 2013). A Latin Hypercube design iteratively sampled the parameter space. The cost function was to minimize overall muscle fatigue as defined by Pedotti *et al.* (Pedotti, 1978), and the center of gravity of the head was constrained to ±5 mm of translation in the x direction and ±0.09 rad of rotation about the y axis. Each simulation was only under gravitational force with T1 fixed, and ran for 0.3 s. This allowed the head to reach equilibrium following the initial muscle contractions. Once the optimal neck activation levels were determined, intervertebral forces and moments were extracted with LS-PrePost, and combined using Equation 1, a combined loading criterion derived from PMHS testing that normalizes axial loading and bending moments to values corresponding to 50% risk of cervical spine AIS ≥ 2 injuries (Bass, 2006). CL is the combined loading value, F_z is the peak intervertebral axial force in Newtons, and M_y is the peak intervertebral anterior/posterior moment in Newton-meters.

$$CL = \frac{F_z}{5430} + \frac{M_y}{141} \quad (1)$$

Dynamic Simulations

Three dynamic scenarios summarized in Table 1 were simulated for each location in Figure 1 and masses of 0, 3, and 5 kg. The muscle activations derived from the static optimizations were used for each scenario to provide realistic conditions before impact. Three militarily relevant scenarios were used to simulate a range of kinematic exposures. First, to simulate running the first dynamic scenario provided a vertical 1 g half sine acceleration pulse over 500 ms to T1. Second, jumping from an elevated platform such as a helicopter or ledge was simulated by providing a vertical 4 g half sine acceleration pulse over 100 ms to T1. Third, a free fall parachute opening was simulated by providing a horizontal 10 g acceleration pulse over 50 ms to T1. For each simulation, the vertebral location and magnitude of the peak intervertebral forces, moments, and combined loads were determined using LS-PrePost and a custom Matlab analysis suite written by the authors.

Table 1: Summary of Dynamic Simulation Inputs

Scenario	Peak Accel. (g)	Duration (ms)	Direction
Running	1	500	+Z
Jumping	4	100	+Z
Parachute Opening	10	50	-X

Injury Criterion

There currently is no injury criterion available for chronic intervertebral disk (IVD) degeneration due to repetitive loading. However, Schmidt et al. developed an injury criterion for bony fracture of the lumbar spine due to cyclic loading that uses an effective stress and R value as determined by ISO 2361-5 (Organization, 2004, Schmidt, 2012). For this study, peak effective stress was determined by dividing the peak intervertebral force by an IVD cross sectional area of 0.000358 m^2. This number was determined using MicroCT images to measure the IVD cross sectional area of C2-C3 through C7-T1 for 22 PMHS that were then averaged. The R value is calculated using Equation 2, where S_{pe} is the peak effective stress of the scenario, S_{ut} is the acute ultimate strength of the cervical spine, c is the static stress in the neck due to gravitational loading, L is years of exposure, and N is number of exposures per year.

$$R = \left(L \left(\frac{S_{pe} * N^{\frac{1}{6}}}{S_{ut} - c} \right)^6 \right)^{\frac{1}{6}} \quad (2)$$

To adapt the formulation of Schmidt et al. to the cervical spine, the ultimate strength used was 4830N (Mertz et al. (Mertz, 2003)) and converted to stress using the average IVD cross sectional area. Static simulations without a head supported mass were used to derive a value of 0.0483 MPa for c. A career length of 1 year was used for L because significantly more violent impacts were used in the development of this criterion (Organization, 2004), and consultation with military operators determined that yearly exposures were 3hrs a day 2 days a week of 1Hz running, a typical 5 jump landings per day 5 days a week, and up to 100 parachute jumps per year.

RESULTS

Static Optimization Results

Figure 2 provides the effective stress and combined loading results from the static optimization tests. There was no trend between mass or mass location for the resulting force, moment, and combined loading values in the osteoligamentous spine. The values with the additional head supported mass are higher than when no mass is applied. Values increase with increasing X distance from the CG, but a more subtle trend appears with increasing Z distance from the CG. Remaining at the X-coordinate of the CG while increasing the Z distance has little effect on the loading values. However, as the X-distance from the CG increases, increasing the Z-distance from the CG decreases the loading values. The range of stress is 1.37 MPa and the range of combined loading is 0.112.

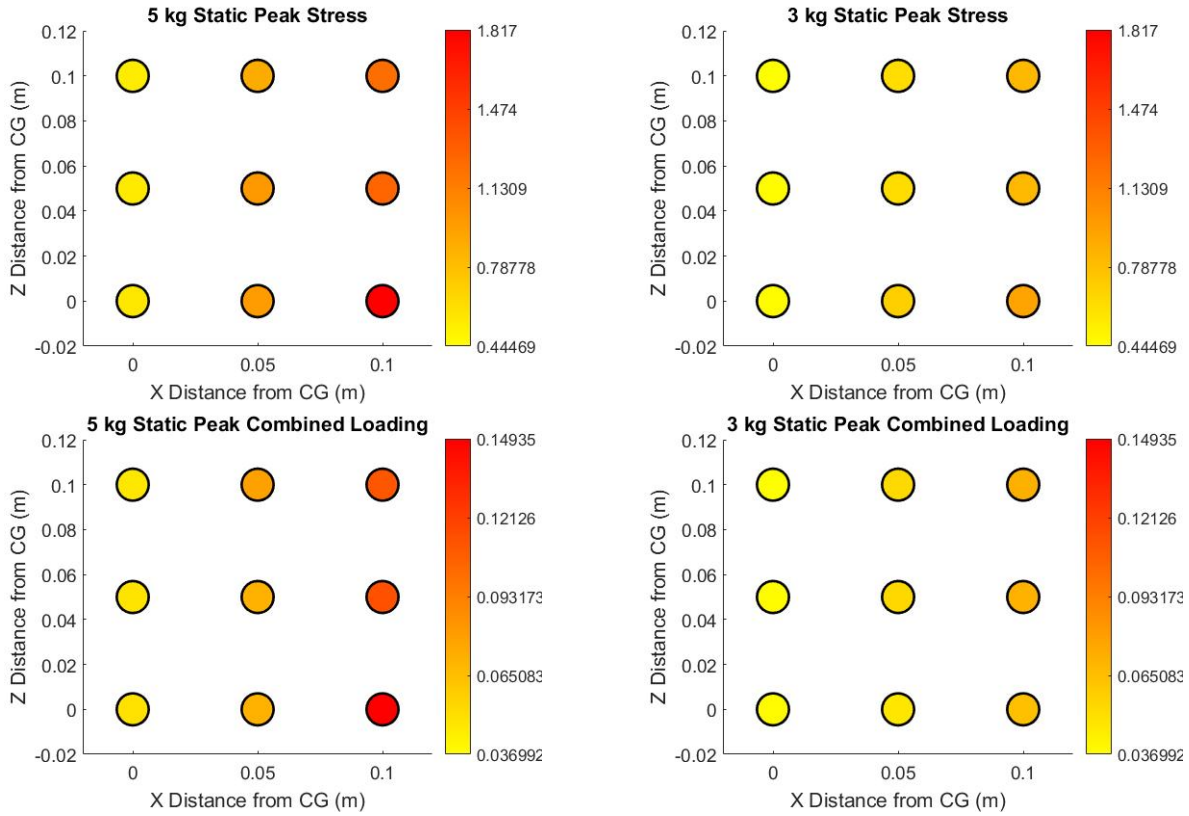

Figure 2: Heat map illustrations of the peak intervertebral effective stresses (MPa) amd peak effective combined loading values for statically supporting the head mass under gravity. Stresses generally increase with increasing X-distance of head supported mass from the head CG.

Dynamic Simulation Results

Figure 3 illustrates the maximum effective intervertebral stresses by location for the three scenarios and two masses. In each plot, the minimum and maximum value has been changed to line up with that particular scenario in order to highlight the impact of location. There is an apparent trend for all actions that moving head supported mass further in the X direction from the head CG results in higher intervertebral stresses. However for parachute openings, there appears to be an additional trend that moving head supported mass further in the Z direction decreases effective stresses. The peak effective stress values for the 5 kg mass are 2.66, 3.42, and 3.30 MPa for running, jumping, and parachute openings respectively, and for the 3 kg mass are 1.49, 2.54, and 2.66 MPa for running, jumping, and parachute openings respectively. The maximum stresses of the dynamic scenarios without head supported mass were 0.66, 1.06, and 0.84 MPa for the running, jumping, and parachute opening scenarios respectively.

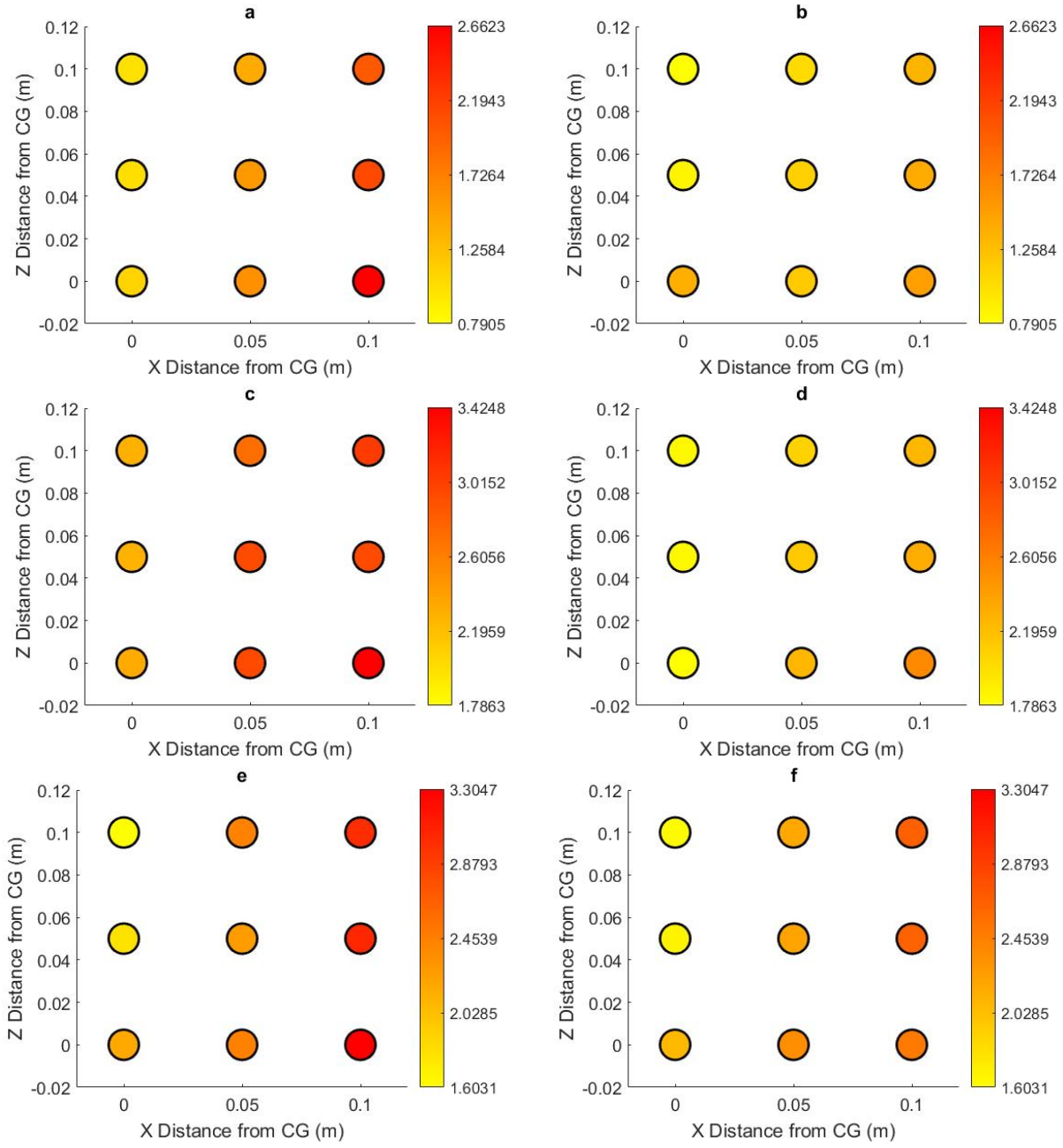

Figure 3: Heat map illustrations of the maximum intervertebral effective stresses (MPa) of the six combinations of mass and dynamic scenarios: a) 5 kg running b) 3 kg running c) 5 kg jumping d) 3 kg jumping e) 5 kg parachute opening f) 3 kg parachute opening. Stresses generally increase with increasing X-distance of head supported mass from the head CG.

Figure 4 illustrates combined loading by location for the three scenarios and two masses. Each plot has the minimum and maximum value optimized to highlight the impact of location. The combined loading value increases as the X-distance from the head CG increases. For parachute openings, there appears to be an additional trend that moving head supported mass further in the Z direction decreases effective stresses. The combined loading values for the parachute opening

are higher than jumping. The peak combined loading values for the 5 kg are 0.25, 0.34, and 0.38 for running, jumping, and parachute openings respectively, and 0.15, 0.24, and 0.32 for running, jumping, and parachute openings respectively for 3 kg. The maximum combined loading values for the dynamic scenarios without head supported mass are 0.05, 0.10, and 0.13 for the running, jumping, and parachute opening scenarios.

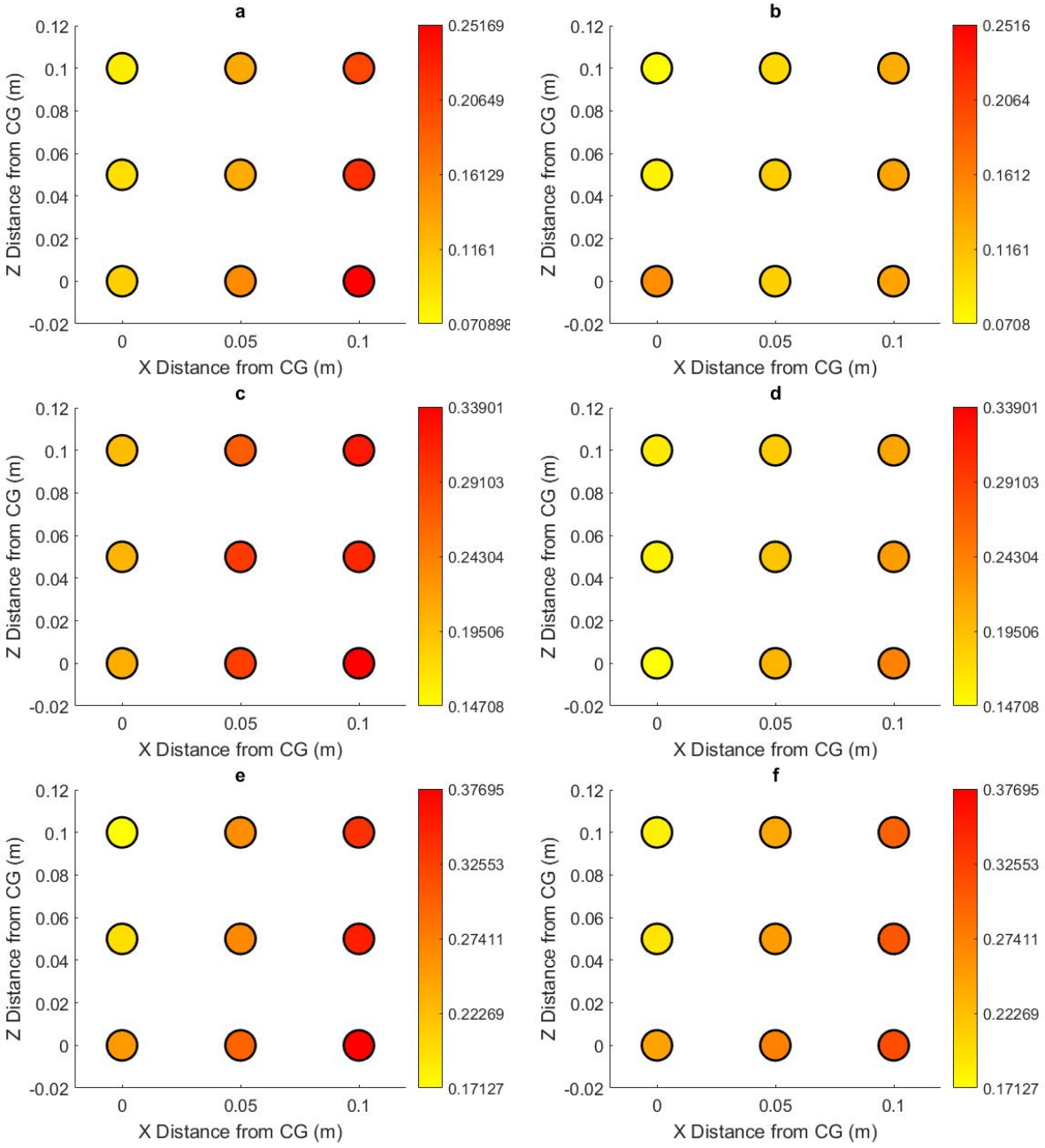

Figure 4: Heat map illustrations of the maximum intervertebral combined loading values of the six combinations of mass and dynamic scenarios: a) 5 kg running b) 3 kg running c) 5 kg jumping d) 3 kg jumping e) 5 kg parachute opening f) 3 kg parachute opening.

Figure 5 illustrates the R value for repeated motion injury adapted for cervical spine repeated motion injury as calculated using Equation 2. Since this value is calculated using the maximum effective stress, the calculated values increase with increasing X-distance from the CG values. A key difference in the R value from the results above is that the running has significantly higher values relative to the other scenarios since the repeated exposure is much larger than the career assumptions for jumping and parachute shock.

Figure 6 shows iso-contours for R = 0.4 for X excursions (horizontal) of the head supported mass from the head center of gravity. For X-distance from the CG there is a strong dependence between risk and excursion.

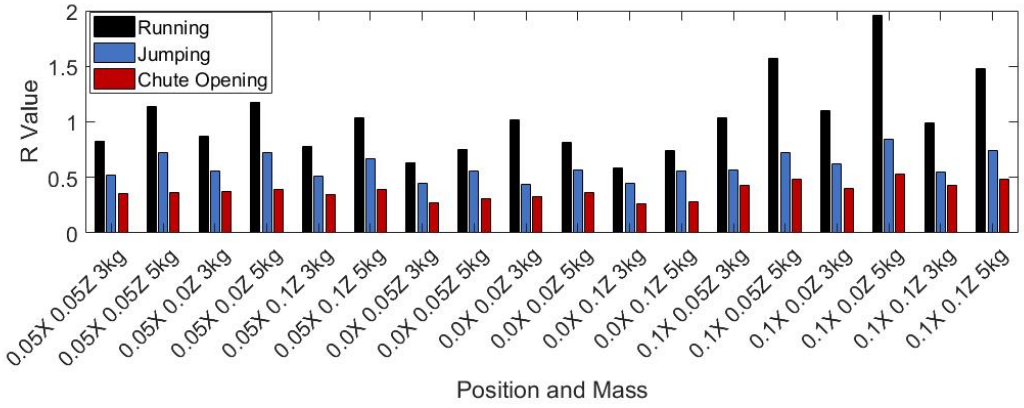

Figure 5: Calculated R values from ISO 2361-5 on vibrational loading.

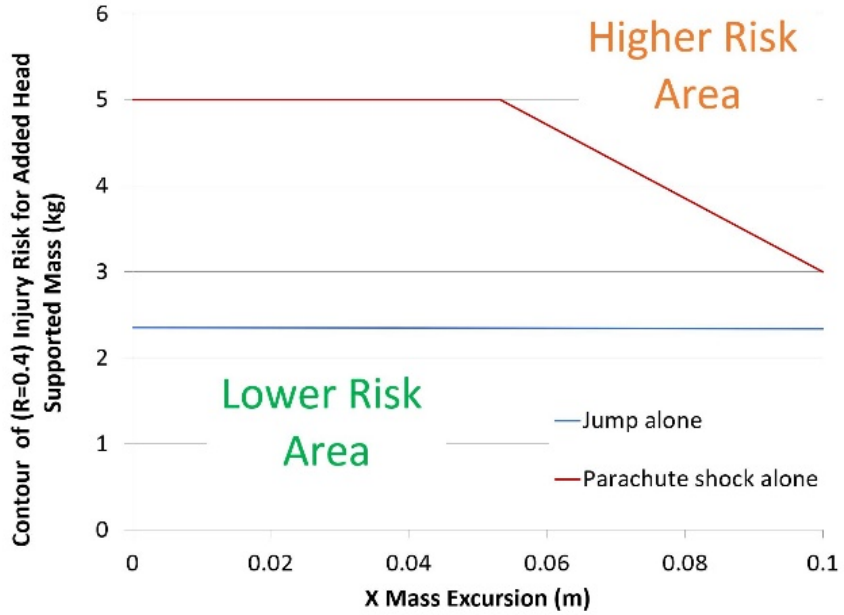

Figure 6: Iso-risk contour plots of mass vs excursion distance for R = 0.4. X-direction added head mass center of gravity excursion. The slope of the contour lines indicate X-distance excursions have an influence on injury risk.

DISCUSSION

The data does support the first hypothesis that forces generated by the cervical musculature in the static loading scenarios would be a significant portion of the forces experienced in the dynamic scenarios. The static stresses account for 30 – 70% of the peak dynamic stresses. This makes sense because the increased stresses within the neck are due to three key factors: increased load under gravity, increased muscle activation to support the load, and increased dynamic inertial loading. These results show that inertial loading results in only a fraction of the intervertebral stresses, and the static loading may be a key contributing factor to chronic injury.

The results partially supported that distance increases between the location of the applied load and the head's CG result in increased intervertebral stress and combined loadings for dynamic scenarios. The trend was seen in the X-direction but not the Z-direction even for the parachute openings where the acceleration was transverse to the cervical spine. These results are illustrated in the field, where anecdotal evidence shows Special Operations Combat Soldiers prefer to carry night vision systems directly above their head CG when not in use. This is most likely attributed to two aspects. First, increasing X-distance of the head supported mass increases the moment about the OC joint because it is perpendicular to the loading vector. This not true for increasing the Z-distance. The second is the non-linearity of muscle loading curves. Mass added further from the CG in the X-direction, requires higher extensor activation to balance the increased moment. This increased activation moves the extensor muscles further up the loading curve, resulting in higher generated forces for a given displacement. Therefor higher dynamic intervertebral forces will be generated by increasing the head supported mass' X-distance from the head CG but not Z-distance. The results also showed that increasing the Z-distance of the head supported mass for a given X-distance away from the CG decreased the loading values. This is because increasing the Z-distance of the head supported mass decreases the X-distance of the overall CG for the head/head supported mass system, allowing the phenomenon described above to take effect.

To support the hypothesis that stresses due to increased head supported mass indicate the potential for repetitive loading injury, an injury criterion developed for lumbar fatigue loading endplate fracture by Schmidt et al. using a meta-analysis of multiple PMHS repetitive loading studies was used (Schmidt, 2012). Based on the S-N fatigue failure curves provided by Schmidt et al. the lower stresses experienced in the running scenario would require between 1000 – 1 million cycles to reach the 50 percent injury risk contour of a 20 year old male. Jumping and parachute opening stresses would require 50-50,000 cycles to reach the 50 percent injury risk curve of a 20 year old male. Both of the cycle numbers are reasonable career exposures, particularly for some of the Special Operations Combat Soldiers. The R values tell a similar story, with running values between 0.7 and 1.9 indicating 10 - 80 percent risk of injury for males. However, because the R value is dependent on exposure, these R values are rather unreliable to due inexact exposure calculations. These exposure values were based on anecdotal interactions with a Special Operations Combat Soldier. Furthermore, this exposure only accounts for three activities, not all of the actions with a head supported mass. Also, each of the three exposures were treated as isolated and their interaction was not taken into account. The true R values would be expected to be higher and requires a more robust understanding of the exposure to determine.

There were several limitations in this study. First, the lack of a suitable injury criterion for the cervical spine. The criterion from Schmidt et al. (Schmidt, 2012) was formulated using data for endplate fracture in the lumbar spine, not soft tissue deterioration in the cervical spine. Also, the criterion was built on data collected from PMHS fatigue tests that do not take into account healing. The R value calculation is supposed to take into account changes in strength properties as the spine deteriorates. However, due to a lack of available data on the deterioration of the cervical spine, a constant ultimate stress was used, which is conservative for repeated motion injury. Furthermore, input kinematics were idealized for the scenarios selected. Intervertebral stresses were calculated using an average of the peak force over the entire cervical spine IVD. This is not entirely realistic, particularly in the bending modes seen in some of the simulations. However Schmidt et al. (Schmidt, 2012) used a similar calculation for the effective stress, making comparisons to those values suitable. The final limitation was the limited number of mass and location values for the head supported mass.

CONCLUSIONS

This study provided a novel insight into the role of head supported mass on intervertebral loads and their implications for chronic cervical spine injuries. We found that loads increase as the head supported mass increases, and as the CG of the applied load is moved in the X direction away from the CG of the head. While loads from running or jumping with a head supported mass have low potential for injury, loads caused by violent events such as parachute openings may increase the risk for chronic cervical spine injury. This study lays the foundation for future work to build robust design guidance envelopes to reduce chronic injury risk for head supported mass and center of gravity location in terms of career longevity and assumed occupational scenarios under repeated impact loading. Such design guidelines are increasingly necessary as military requirements may increase head supported mass.

REFERENCES

ARBOGAST, K. B., S. BALASUBRAMANIAN, T. SEACRIST, M. R. MALTESE, J. F. GARCIA-ESPANA, T. HOPELY, E. CONSTANS, F. J. LÓPEZ-VALDÉS, R. W. KENT AND H. TANJI (2009). Comparison of kinematic responses of the head and spine for children and adults in low-speed frontal sled tests, SAE Technical Paper.

BASS, C., L. DONNELLAN, R. SALZAR, S. LUCAS, B. FOLK, M. DAVIS, K. RAFAELS, C. PLANCHAK, K. MEYERHOFF AND A. ZIEMBA (2006). A new neck injury criterion in combined vertical/frontal crashes with head supported mass. 2006 international IRCOBI conference on the biomechanics of impact.

BUTLER, B. P. (1996). Long-Duration Exposure Criteria for Head-Supported Mass, ARMY COMMAND AND GENERAL STAFF COLL FORT LEAVENWORTH KS.

CAMACHO, D. L., R. W. NIGHTINGALE, J. J. ROBINETTE, S. K. VANGURI, D. J. COATES AND B. S. MYERS (1997). Experimental flexibility measurements for the development of a computational head-neck model validated for near-vertex head impact, SAE Technical Paper.

CHANCEY, V. C., R. W. NIGHTINGALE, C. A. VAN EE, K. E. KNAUB AND B. S. MYERS (2003). "Improved estimation of human neck tensile tolerance: reducing the range of reported tolerance using anthropometrically correct muscles and optimized physiologic initial conditions." Stapp Car Crash Journal **47**: 135.

CHANCEY, V. C., D. OTTAVIANO, B. S. MYERS AND R. W. NIGHTINGALE (2007). "A kinematic and anthropometric study of the upper cervical spine and the occipital condyles." Journal of biomechanics **40**(9): 1953-1959.

DIBB, A. T. (2011). Pediatric Head and Neck Dynamic Response, Duke University.

DIBB, A. T., C. A. COX, R. W. NIGHTINGALE, J. F. LUCK, H. C. CUTCLIFFE, B. S. MYERS, K. B. ARBOGAST, T. SEACRIST AND C. R. BASS (2013). "Importance of muscle activations for biofidelic pediatric neck response in computational models." Traffic injury prevention **14**(sup1): S116-S127.

DIBB, A. T., H. C. CUTCLIFFE, J. F. LUCK, C. A. COX, B. S. MYERS, C. R. BASS, K. B. ARBOGAST, T. SEACRIST AND R. W. NIGHTINGALE (2014). "Pediatric head and neck dynamics in frontal impact: Analysis of important mechanical factors and proposed neck performance corridors for 6-and 10-year-old ATDs." Traffic injury prevention **15**(4): 386-394.

DVORAK, J., M. PANJABI, J. NOVOTNY AND J. ANTINNES (1991). "In vivo flexion/extension of the normal cervical spine." Journal of Orthopaedic Research **9**(6): 828-834.

EAGLE, S. R., T. NAGAI, P. MORGAN, R. HENDERSHOT AND T. C. SELL (2017). "Naval Special Warfare (NSW) crewmen demonstrate diminished cervical strength and range of motion compared to NSW students." Work **58**(2): 111-119.

EWING, C. L. AND D. J. THOMAS (1972). Human Head and Neck Response to Impact Acceleration, NAVAL AEROSPACE MEDICAL RESEARCH LAB PENSACOLA FL.

MANOOGIAN, S. J., E. A. KENNEDY AND S. M. DUMA (2005). A Literature Review of Musculoskeletal Injuries to the Human Neck and the Effects of Head-Supported Mass Worn by Soldier, ARMY AEROMEDICAL RESEARCH LAB FORT RUCKER AL.

MANOOGIAN, S. J., E. A. KENNEDY, K. A. WILSON, S. M. DUMA AND N. M. ALEM (2006). "Predicting neck injuries due to head-supported mass." Aviation, space, and environmental medicine **77**(5): 509-514.

MERTZ, H. J., A. L. IRWIN AND P. PRASAD (2003). Biomechanical and scaling bases for frontal and side impact injury assessment reference values, SAE Technical Paper.

ORGANIZATION, I. S. (2004). Mechanical vibration and shock - Evaluation of human exposure to whole body vibration. Method for evaluation of vibration containing multiple shocks.

PEDOTTI, A., V. KRISHNAN AND L. STARK (1978). "Optimization of muscle-force sequencing in human locomotion." Mathematical Biosciences **38**(1-2): 57-76.

POZZO, T., A. BERTHOZ AND L. LEFORT (1989). Head kinematic during various motor tasks in humans. Progress in brain research, Elsevier. **80:** 377-383.

SCHMIDT, A. L., G. PASKOFF, B. S. SHENDER AND C. R. BASS (2012). "Risk of lumbar spine injury from cyclic compressive loading." Spine **37**(26): E1614-E1621.

SCHOENFELD, A. J., A. A. GEORGE, J. O. BADER AND P. M. CARAM JR (2012). "Incidence and epidemiology of cervical radiculopathy in the United States military: 2000 to 2009." Clinical Spine Surgery **25**(1): 17-22.

VAN EE, C. A., R. W. NIGHTINGALE, D. CAMACHO, V. C. CHANCEY, K. E. KNAUB, E. A. SUN AND B. S. MYERS (2000). Tensile properties of the human muscular and ligamentous cervical spine, Duke University Durham, NC.

VAN MAMEREN, H., H. SANCHES, J. BEURSGENS AND J. DRUKKER (1992). "Cervical Spine Motion in the Sagittal Plane II: Position of Segmental Averaged Instantaneous Centers of Rotation-A Cineradiographic Study." Spine **17**(5): 467-474.